Delocalizing Trypsin Specificity with Metal Activation†

W. Scott Willett,‡,§ Linda S. Brinen,‖ Robert J. Fletterick,‖ and Charles S. Craik*,‡

Department of Pharmaceutical Chemistry, University of California at San Francisco, San Francisco, California 94143-0446, and Department of Biochemistry and Biophysics, University of California at San Francisco, San Francisco, California 94143-0448

Received December 20, 1995; Revised Manuscript Received March 15, 1996⊗

ABSTRACT: Recognition for proteolysis by trypsin depends almost exclusively on tight binding of arginine or lysine side chains by the primary substrate specificity pocket. Although extended subsite interactions are important for catalysis, the majority of binding energy is localized in the P_1 pocket. Analysis of the interactions of trypsin with the P_1 residue of the bound inhibitors ecotin and bovine pancreatic trypsin inhibitor suggested that the mutation D189S would improve metal-assisted trypsin N143H, E151H specificity toward peptides that have a Tyr at P_1 and a His at P_2'. In the presence of transition metals, the catalytic efficiency of the triple mutant Tn N143H, E151H, D189S improved toward the tyrosine-containing peptide AGP**YAH**SS. Trypsin N143H, E151H, D189S exhibits a 25-fold increase in activity with nickel and a 150-fold increase in activity with zinc relative to trypsin N143H, E151H on this peptide. In addition, activity of trypsin N143H, E151H, D189S toward an arginine-containing peptide, YLVGP**RGH**FYDA, is enhanced by copper, nickel, and zinc. With this substrate, copper yields a 30-fold, nickel a 70-fold, and zinc a 350-fold increase in activity over background hydrolysis without metal. These results demonstrate that the engineering of multiple substrate binding subsites in trypsin can be used to delocalize protease specificity by increasing relative substrate binding contributions from alternate engineered subsites.

The omnipresence of proteases and their naturally occurring macromolecular inhibitors has placed them among the most studied proteins in biochemistry. In addition to their importance in biology and medicine, proteases are of great practical importance. Proteases are therefore an important focus of structural and engineering studies because they have uses ranging from analytical laboratory tools to industrial processing enzymes. For example, subtilisin has been engineered to be an efficient peptide ligase (Abrahmsen et al., 1991) and to have enhanced thermal stability (Braxton & Wells, 1992) as well as increased stability in organic solvents (Arnold, 1993). Both subtilisin and trypsin have been engineered to possess altered specificity through substrate-assisted catalysis (Carter & Wells, 1987; Corey et al., 1995) and by mutation of substrate-contacting regions of the enzymes [for a review, see Perona and Craik (1995)]. Also, tissue-type plasminogen activator (t-PA) has been engineered to be more fibrin-specific in an effort to enhance its value as a therapeutic protease (Paoni et al., 1993). Protease−substrate interactions provide a useful arena in which to test our understanding of macromolecular recognition.

Protease substrate specificity is still incompletely understood, making engineering difficult, yet well-defined principles such as charge and shape complemetarity can be tested experimentally to alter macromolecular recognition. Among the simplest binding determinants to engineer are metal coordination sites for Zn, Ni, or Cu ions because the metalloprotein structural database clearly indicates the preferred distances, geometries, and ligands for these metals. Using structure-based design, histidine specificity through metal coordination has been engineered previously into trypsin for the P_2' position of substrate. This was achieved by creating an intermolecular metal binding site bridging enzyme and substrate so that the enzyme hydrolyzes a tyrosine peptide bond, AGP**Y**−**AH**SS, only in the presence of nickel or zinc (Willett et al., 1995). Tyrosine fits within the trypsin specificity pocket but with poor complementarity, resulting in a buried negative charge at Asp 189. While trypsin N143H, E151H exhibits the designed activity, subsequent efforts have concentrated on improving the design to increase the efficiency of the enzyme and on solving its X-ray crystal structure in the presence of transition metals in an effort to understand the structural context of the observed activity.

Visual analysis of the P_1−S_1 interactions in trypsin and chymotrypsin suggested that a single mutation in trypsin N143H, E151H could improve catalytic activity of the enzyme toward a P_1 tyrosine substrate. Chymotrypsin is specific for large hydrophobic amino acids at P_1, and it contains a serine at position 189 in the bottom of the S_1 subsite. In contrast, trypsin possesses an aspartate at position 189 which is responsible for its activity toward positively charged arginine and lysine substrates. Trypsin D189S has previously been characterized kinetically, and its crystal structure complexed to BPTI was solved (Perona et al., 1994). On the basis of the structure of trypsin D189S and the kinetic information of the two trypsin mutants (N143H, E151H, and D189S), it was reasoned that replacement of Asp 189 in trypsin N143H, E151H with serine as found in chymotrypsin would result in increased metal-dependent

† This work was supported in part by NSF Grant MCB-9219806 to C.S.C. and NIH Grant DK39304-06A2 to R.J.F. W.S.W. was supported by the University of California Biotechnology Research and Education Program.

* Author to whom correspondence should be addressed.

‡ Department of Pharmaceutical Chemistry.

§ Current address: Department of Chemistry and Biochemistry, University of Colorado at Boulder, Boulder, CO 80309.

‖ Department of Biochemistry and Biophysics.

⊗ Abstract published in *Advance ACS Abstracts,* April 15, 1996.

S0006-2960(95)03019-4 CCC: $12.00

catalytic activity of trypsin N143H, E151H, D189S toward the peptide substrate AGP**Y**−**AH**SS. This paper describes the rationale, modeling, and kinetic characterization of these engineered trypsins, and the accompanying paper (Brinen et al., 1996) describes the X-ray structural analysis of the designed metal binding site in trypsin N143H, E151H complexed to a variant of ecotin in which a histidine has been engineered into the P_2' site at position 86, Ec A86H. The pan-specific serine protease inhibitor, ecotin (McGrath et al., 1991, 1994), serves here as a model for bound substrate in order to provide the structural context of the observed catalytic activity of this designed protease.

MATERIALS AND METHODS

Mutagenesis, Expression, and Purification of Trypsin and Ecotin. Materials and methods involving trypsin have been described previously (Willett et al., 1995) and are the same for the experiments reported here. Trypsin N143H, E151H, D189S (subsequently referred to as Tn N143H, E151H, D189S) was constructed by making single-stranded DNA from pST plasmid containing the N143H, E151H mutations and performing site-directed mutagenesis (Kunkel, 1985) using the oligonucleotide GGGAGG**A**AAG**AGTTC**CTGC-CAGGG (bold type denotes mismatch). The ecotin gene was mutated by site-directed mutagenesis to create ecotin A86H (subsequently referred to as Ec A86H) using the noncoding oligonucleotide GGGGCCA**C**AG**C**TGCTAC-TAC**GTG**ACGGGCC. Ec A86H was expressed in *Escherichia coli* strain X90 [F′ *lac I*^{q}, *lac ZY, pro AB*/Δ-(lac-pro), ara, mal A, argEam, thi, rif^r] as described previously (Wang et al., 1995) and purified as follows. The periplasmic fraction from a 1 L culture containing ecotin was passed through a 5 mL DEAE-Sepharose FF (Pharmacia) column equilibrated with 10 mM Tris, pH 8.0. The unbound fraction was collected and made 20 mM in glycine from a 2 M stock solution and then adjusted to pH 3.0 for cation-exchange chromatography on a 15 mL SP-Sepharose FF column (Pharmacia). The ecotin was eluted from the resin with a 75 mL gradient of 0−1.5 M NaCl in 20 mM glycine, pH 3.0. Fractions containing ecotin were dialyzed into water and concentrated to ∼500 μM ecotin (ϵ_{280} = 21860 M^{-1}) with a Centriprep 10 concentrator (Amicon). This material was then loaded in 3 mL lots onto a Vydac C4 prep column (2 cm × 20 cm) equilibrated with 0.1% TFA, and ecotin was eluted with a 0−40% acetonitrile/0.1% TFA gradient over 15 min. Fractions containing pure ecotin as judged by Coomassie-stained PAGE were lyophilized, resuspended in water, reconcentrated with a Centricon 10 (Amicon) to ≥1 mM, and stored at 4 °C.

Computer Modeling of Trypsin−Substrate Interactions. The original model for the metal binding site at P_2' was created using the crystal structure of trypsin complexed to bovine pancreatic trypsin inhibitor (BPTI) displayed on a Silicon Graphics Indigo with the program Insight II (Biosym Technologies, Inc.). Subsequent to that modeling, the gene for the serine protease inhibitor, ecotin, was cloned and expressed, and its X-ray crystal structure was solved complexed to trypsin (McGrath et al., 1994). Availability of the ecotin clone and expression system made it an ideal candidate for use as a substrate model in these studies. Hence, the model of the P_2' His metal binding site at positions 143 and 151 was recreated using the ecotin/trypsin crystal structure. Modeling of the metal binding site was performed as before on a Silicon Graphics Indigo machine running Insight II. Modeling of tyrosine in the P_1 position bound to Tn N143H, E151H, D189S was performed by displaying the trypsin/ecotin H143/151/P_2'-His model coordinates and changing the P_1-Met of ecotin to Tyr and Asp 189 of trypsin to Ser. The tyrosine side chain rotamer was adjusted to eliminate any sub van der Waals contacts, and the Ser189 side chain was rotated to the position found in the crystal structure of Tn D189S complexed to BPTI (Perona et al., 1994). Superpositions of the models were performed with subroutines of Insight II using the Cα and liganding nitrogen atoms of the histidines at P_2', 143, and 151 (12 atoms total). Main chain movements were not allowed in the modeling, nor were any energy minimization calculations performed.

Kinetic Parameter Determination. Kinetic parameter determination of the AGPYAHSS peptide and synthetic substrate hydrolysis was described previously (Willett et al., 1995). For the case of Tn N143H, E151H, D189S, 100 nM enzyme was used in the peptide assay. All peptide assays were carried out in 5 mM PIPPS, 1 mM Tris, 100 mM NaCl, and 1 mM $CaCl_2$, pH 8.0 at 37 °C. In order to quantify the product peaks, the HPLC assay for cleavage of YLVG-P**R**G**H**FYDA was modified from that described for AG-PYAHSS by increasing the gradient from 0−30% acetonitrile in 2.5 min to 0−40% acetonitrile in 3.2 min. For all HPLC assays, 0.001% dimethylformamide was used as an internal standard for quantification of peak areas. Kinetic parameters were calculated by fitting the data to the Michaelis−Menten equation. Crystallization of the complex of Tn N143H, E151H with Ec A86H and the metal soaks are described in detail in the accompanying paper.

RESULTS

Comparison of BPTI and Ecotin Models. Figure 1 shows the three-dimensional location of the engineered metal binding site in the complex of trypsin N143H, E151H bound to ecotin A86H. The trypsin−ecotin complex was used as a model of bound substrate rather than a trypsin−BPTI complex because ecotin has revealed a property of conformability to the structure of the surface of the protease to which it is bound, thereby mimicking substrate interactions over 11 amino acids (J. Perona, C. Tsu, R. Fletterick, and C. S. Craik, unpublished results). Furthermore, an exceptional expression system is available for mutation and expression of variant ecotin inhibitors (McGrath, 1991). To ensure that ecotin was a suitable substrate model, the same modeling that was performed on the trypsin−BPTI complex to design the metal binding site (Willett et al., 1995) was performed with the trypsin−ecotin coordinates. A computer program was used to model a metal binding site that would bridge substrate and enzyme using geometric and bond distance criteria. The coordinates of the trypsin−ecotin complex were searched for residues that could be replaced with histidine to form a potential metal binding site (Willett et al., 1995; Higaki et al., 1989, 1990). No energy minimization calculations were performed in the modeling. The results of the computer search were displayed using Insight II, and the conformations of the His side chains were adjusted manually to optimize the metal binding distances and geometries. Figure 2 shows a comparison of the trypsin−ecotin and trypsin−BPTI complexes. These two models are strikingly similar at their active site, even though the two inhibitor

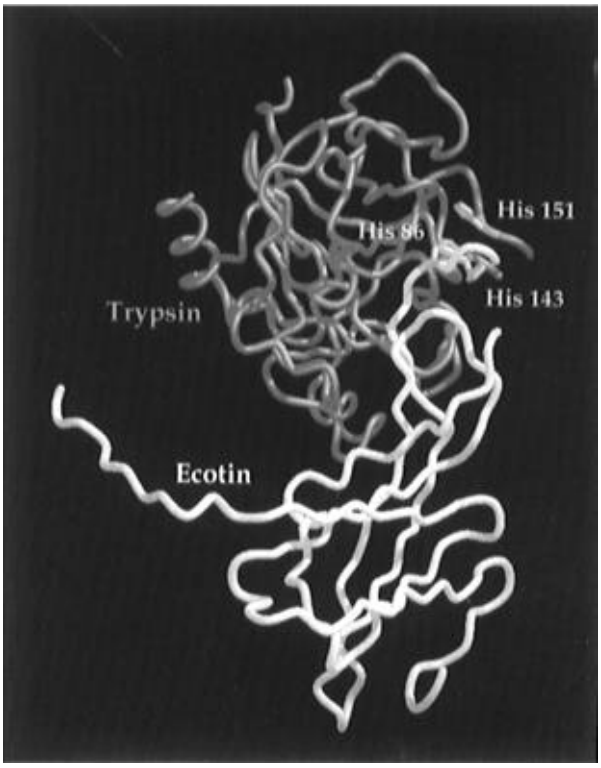

FIGURE 1: Location of the engineered metal binding site in trypsin N143H, E151H bound to ecotin A86H. A single ecotin−trypsin heterodimer (E_1-T_1) is shown for clarity.

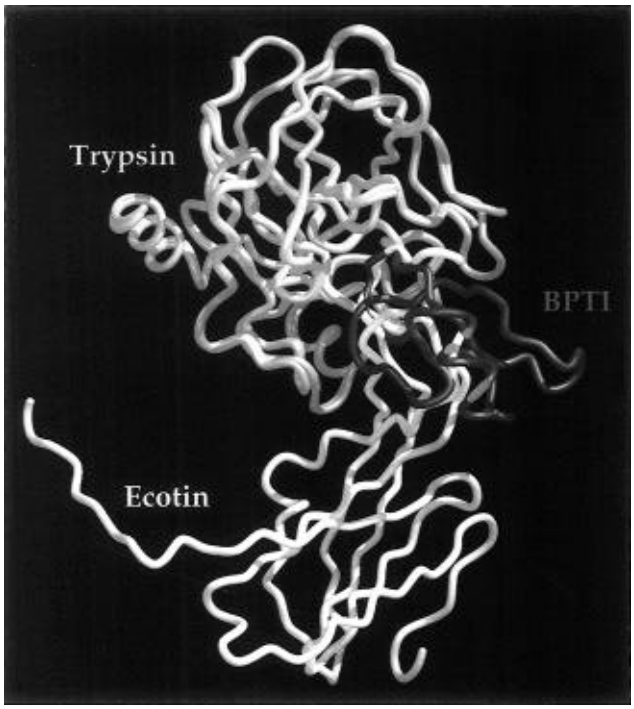

FIGURE 2: Superposition of trypsin−BPTI and trypsin−ecotin complexes showing the structural similarity of enzyme−inhibitor interfaces near the active site of trypsin.

molecules are unrelated in sequence and three-dimensional structure. This similarity supports the use of these macromolecules as peptide substrate models because they bind in extended β-strands across the surface of the enzyme, much the way a peptide lacking secondary structure might. The Cα and metal-liganding atoms of the histidines in the two models superimpose with an RMS deviation of 1.0 Å. The coordination geometry of each model can best be described

Table 1: Comparison of BPTI and Ecotin Models

parameter	BPTI model	ecotin model
distances (Å)[a]		
P_2'-His Nε2−M^{2+}	1.9	2.0
H143 Nε2−M^{2+}	2.0	2.1
H151 Nx−M^{2+}	1.6 (ε2)	2.0 (δ1)
angles (deg)[b]		
143−metal−151	119	112
151−metal−P_2'	123	78
P_2'−metal−143	105	99
metal−imidazole planarity (deg)[c]		
P_2'-His	160	175
His 143	140	170
His 151	−115	−168
His rotamers (deg)[d]		
P_2'-His χ_1	−175	−173
P_2'-His χ_2	−49	−67
His 143 χ_1	−70	−60
His 143 χ_2	−175	145
His 151 χ_1	−35	−150
His 151 χ_2	17	111

[a] Distances are measured between the Nε2 atom of the indicated histidine residue and the metal ion (M^{2+}). [b] Angles are measured between the Nε2 atoms of the indicated histidine residues and the metal ion. [c] The planarity of the metal ion with the imidazole ring of the histidine is measured with the dihedral angle formed by the Cγ, Cδ2, Nε2, and metal atoms. A dihedral angle of ±180° represents a metal ion that is coplanar with the imidazole ring. [d] χ_1 is defined as the dihedral angle formed by the N, Cα, Cβ, and Cγ atoms of histidine, and χ_2 is formed by the Cα, Cβ, Cγ, and Nδ1 atoms.

as distorted tetrahedral, based on only three ligands. The fourth ligand is assumed to be water in each case, positioned in bulk solvent away from the protein surface. The most important difference between the two models is that His 151 of trypsin in the trypsin−ecotin complex is coordinated to the metal ion through Nδ1. In contrast, His 151 of trypsin in the trypsin−BPTI complex is predicted to bind metal through Nε2. Scrutiny of His 151 in the trypsin−BPTI complex model reveals its poor geometry: the Nε2−metal bond length is only 1.6 Å, and the metal ion is predicted to bind 65° out of the plane of the imidazole ring. This very short bond distance and large deviation out of the ring plane (30° tolerance is observed in most metalloproteins; Chakrabarti, 1990; Christianson & Alexander, 1989) suggest a poor fit. The ecotin−trypsin model displays somewhat better metal binding geometry with His 151 as the metal ion is predicted to bind 2 Å from Nδ1 and only 12° out of the ring plane. The histidine rotamers are all close to the preferred rotamers for those side chains (Ponder & Richards, 1987) and make no sub van der Waals contacts with any other parts of the complex. Table 1 summarizes the metal binding site parameters for the two models.

Modeling of Tyrosine and Serine in the P_1 Pocket of Trypsin. A P_1 tyrosine was modeled into ecotin at position 84 (Ec M84Y), and a serine was modeled into trypsin at position 189 (Tn D189S). The Tn N143H, E151H−ecotin A86H model was used in order to assess the feasibility of constructing the triple trypsin mutant N143H, E151H, D189S as an improved enzyme for metal-regulated AGPY−AHSS hydrolysis. Figure 3 illustrates the results of that modeling, showing the trypsin active site with bound substrate. The catalytic triad is shown with Ser 195 poised to attack the carbonyl carbon of the P_1-Tyr, and the oxyanion hole comprising the backbone nitrogens of Gly 193 and Ser 195 is indicated in blue. The P_1-Met of ecotin was replaced with a tyrosine, and the Tyr rotamer was manually adjusted to

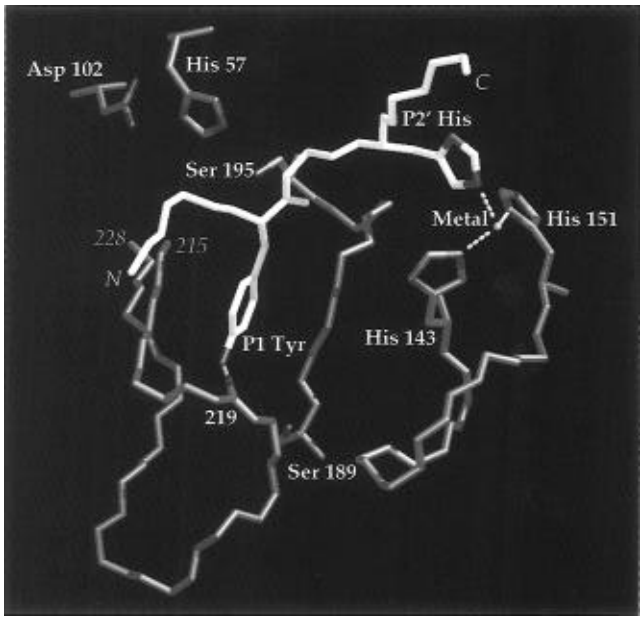

FIGURE 3: Model of P_1-Tyr/P_2'-His substrate bound to Tn N143H, E151H, D189S. This model shows the feasibility of binding a tyrosine substrate (pink) in the S_1 subsite of Tn N143H, E151H, D189S (gray). A hydrogen bond between the P_1-Tyr and Gly 219 carbonyl is shown as a yellow line, as are the metal coordination bonds to the three histidines. The catalytic triad of trypsin is shown with the Ser 195 hydroxyl poised to attack the P_1-Tyr carbonyl carbon and the scissile bond carbonyl oxygen pointing toward the oxyanion hole comprising the backbone nitrogens of Gly 193 and Ser 195.

eliminate sub van der Waals interactions with other residues in the pocket. This was easily achieved so that there were no unfavorable contacts, and a potential short hydrogen bond was formed at 2.7 Å between the Tyr hydroxyl group and the trypsin Gly 219 carbonyl oxygen. When the tyrosine is placed in the P_1 position, the Asp 189 carboxylate oxygens are 3.5 and 5.0 Å from the Tyr hydroxyl group. Although hydrogen bond interactions between Asp or Glu and Tyr are found in other protein structures, given the full negative charge on Asp 189 in the trypsin P_1 pocket, the 3.5 Å interaction with an uncharged P_1-Tyr may be deleterious to substrate binding.

The crystal structure of Tn D189S showed that, apart from the mutation at position 189, the structure of the S_1 subsite in this trypsin variant is identical to that of trypsin (Perona et al., 1994). Serine was placed at position 189 in the orientation found in Tn D189S ($\chi_1 = 53°$), where it makes no sub van der Waals contacts with the surrounding residues. The rotamer ($\chi_1 = 68°$, pdb file 4CHA) of Ser 189 found in α-chymotrypsin makes no unfavorable contacts in the S_1 subsite of trypsin other than with one bound water and so is also a possibility for this model. In either the Tn D189S or chymotrypsin orientation, the Oγ of Ser 189 is 4.8−5.5 Å from the P_1-Tyr hydroxyl group, suggesting that there would be no hydrogen bond energy contributed to binding a P_1-Tyr by Ser 189, unless bridged by solvent.

The model indicates that (1) the S_1 subsite of trypsin can accommodate a tyrosine with no unfavorable contacts and (2) the substitution of a serine at position 189 may result in a more favorable environment for the tyrosine side chain when compared with Asp at position 189 due to removal of the buried negative charge.

Kinetic Characterization of Tn N143H, E151H toward P_1-Arg Substrates. Metal-assisted histidine specificity was previously reported (Willett et al., 1995) demonstrating that the engineered Tn N143H, E151H will hydrolyze tyrosine peptide bonds in the presence of nickel or zinc as long as a histidine is present at the P_2' position of the substrate. Because trypsin normally cleaves Lys or Arg residues, the question remained as to whether a similar increase in activity would be observed for an Arg-X-His-containing peptide. The peptide YLVGP**R**G**H**FYDA, with an Arg at P_1 and a His at P_2', was used to address this question. The longer peptide (compared to AGPYAHSS) was used because it possesses suitable solubility and spectroscopic properties. At high concentrations, transition metals inhibit trypsin, with Zn being the poorest inhibitor. HPLC analysis of the cleavage products (data not presented) shows that 500 μM Cu inhibits cleavage by 90%, 500 μM nickel by 80%, and 500 μM zinc by 20% as determined by percent hydrolysis of the peptide over 30 min. These results are all ±10%. Metals at 500 μM were optimal for observing the sensitivity of the enzyme to metal inhibition. Metal ions in the activity buffer were not soluble for prolonged periods (>1 week) at concentrations greater than 500 μM. These results were compared to experiment with the same metal binding His substrate but using Tn E151Q. This variant was shown previously to be a non-metal-activated protease with wild-type activity against P_1-Arg substrates (Willett et al., 1995). Tn E151Q hydrolysis of YLVGPR−GHFYDA was 90% inhibited by 500 μM copper and only 20% inhibited by both 500 μM nickel and 500 μM zinc, indicating that the metals are interacting with the enzyme−substrate complex in a nonspecific manner. Metal ion inhibition experiments were also performed using the fluorogenic substrate Z-GPR-AMC which contains no amino acid residues C-terminal to the scissile bond and so would be insensitive to metal-mediated effects at the P_2'−S_2' interface. The results of these experiments reveal that copper at 500 μM inhibits Tn N143H, E151H hydrolysis of this fluorogenic substrate by 80%, nickel by 30%, and zinc by 40%. Tn E151Q is inhibited 50% by copper, 10% by nickel, and 25% by zinc.

These data indicate that (1) copper, nickel, and zinc do not activate cleavage of an arginine peptide bond by Tn N143H, E151H, rather they inhibit catalysis, and (2) copper nonspecifically inhibits both proteases 2−5 times more than does nickel or zinc. This inhibition is observed with Z-GPR-AMC as well as the dodecapeptide, YLVGP**R**G**H**FYDA.

Effect of Asp 189 on Metal-Dependent Specificity. Previous studies have shown that removing the negative charge, Asp 189, in the S_1 subsite of trypsin and replacing it with the serine found in that position in chymotrypsin reduces the activity of the enzyme (Tn D189S) by 10^4 on *p*-nitroanilide tripeptide substrates (Perona et al., 1994). Trypsin N143H, E151H, D189S was made with the goal of increasing metal-assisted specificity toward the tyrosine peptide bond in AGPYAHSS. At the same time, it was reasoned that removal of the negative charge in the bottom of the pocket would reduce activity toward a P_1-Arg substrate. Metal-assisted specificity of Tn N143H, E151H, D189S toward a peptide with a P_1 Arg and a P_2'-His would demonstrate that the main specificity determinant for this enzyme is shifted from the P_1 position, to both the P_1 and P_2' position, and that efficient hydrolysis is metal-dependent.

The results of the kinetic analysis of peptide hydrolysis by Tn N143H, E151H, D189S are summarized in Tables 2 and 3. Figure 4 shows the metal titration of activity of Tn

Table 2[a]

enzyme	substrate	k_{cat}/K_m (μM^{-1} min^{-1}) +Cu	+Ni	+Zn	no metal
Tn N143H, E151H, D189S	AGPYAHSS	0.001	0.02	0.24	<0.0008
Tn D189S	AGPYAHSS	0.001	0.001	0.002	<0.0008
chymotrypsin	AGPYAHSS	n/a	n/a	n/a	0.37

[a] Metal concentrations are 200 μM. Errors are ±30%.

Table 3[a]

enzyme	substrate	V_i (μM/min) +Cu	+Ni	+Zn	no metal
TnN143H, E151H, D189S	YLVGPRGHFYDA	0.03	0.07	0.35	0.001
Tn D189S	YLVGPRGHFYDA	0.001	0.002	0.002	0.001

[a] Metal concentrations are 200 μM. Errors are ±30%.

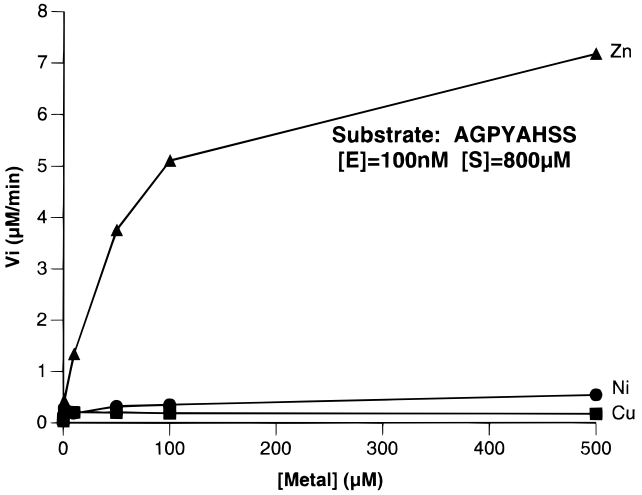

FIGURE 4: Copper, nickel, and zinc titration of activity of Tn N143H, E151H, D189S against the peptide substrate AGPYAHSS. Activity is measured as the initial rate of hydrolysis, V_i (μM/min), at [E] = 100 nM and [S] = 800 μM at T = 37 °C.

N143H, E151H, D189S against 800 μM AGP**Y**−**AH**SS from 0 to 500 μM metal as measured by the initial rate of hydrolysis, V_i (μM/min). Baseline hydrolysis without any metal averages 0.05 μM/h. Copper increases the activity 3-fold above baseline hydrolysis and nickel by 10-fold. A dramatic 150-fold increase in activity was observed with 500 μM zinc.

Figure 5 shows the relative activity for hydrolysis of the P_1-Tyr and P_1-Arg peptides AGP**Y**−**AH**SS (Figure 5a) and YLVGP**R**−**GH**FYDA (Figure 5b) by Tn N143H, E151H, D189S and trypsin D189S, with and without 200 μM Cu^{2+}, Ni^{2+}, or Zn^{2+}. Each enzyme exhibited a small amount of baseline activity, V_i = 0.001 ± 0.0005 μM/min, for hydrolysis of these peptides without metal. Figure 5a shows the relative k_{cat}/K_m for each of the enzymes against AGP**Y**A**H**SS. Copper fails to increase the activity of either protease by a value greater than the error of the measurements. Nickel and zinc increase the activity of Tn N143H, E151H, D189S by 25-fold and 300-fold, respectively. In contrast, Tn D189S is not activated by copper or nickel and activated only 2.5-fold by zinc. In addition, a substrate lacking the P_2' histidine, AGPYAASS, is only hydrolyzed at or below the baseline rate by both proteases in all cases.

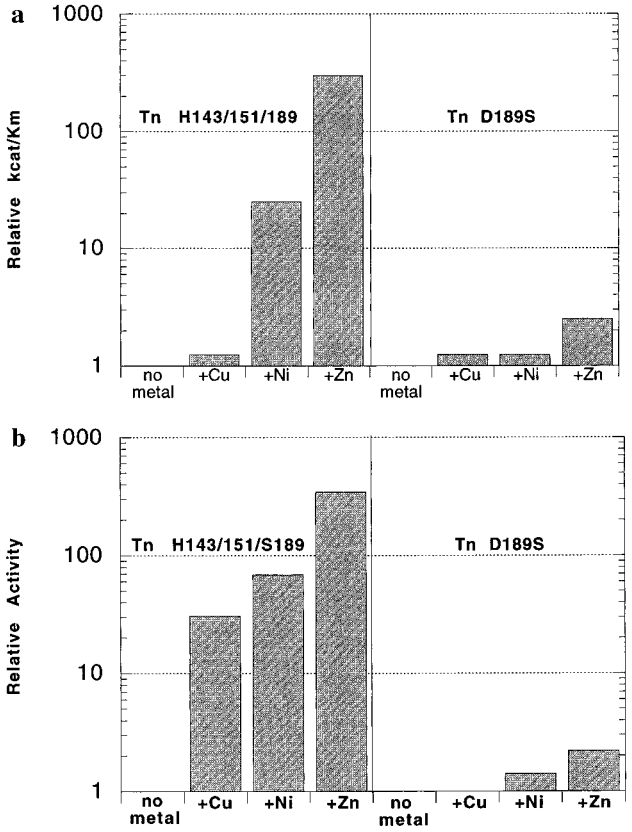

FIGURE 5: Relative activities of Tn N143H, E151H, D189S and Tn D189S against AGP**YAH**SS and YLVGP**RGH**FYDA. Values reported are ±30%. (a) Nickel activates hydrolysis of AGP**YAH**SS by Tn N143H, E151H, D189S by 25-fold, and zinc activates hydrolysis by 300-fold relative to baseline activity with copper, without metal, or by Tn D189S. Only baseline activity was observed for a control substrate, AGPYAASS, lacking the $P2'$ histidine. (b) Activity of Tn N143H, E151H, D189S against YLVGP**RGH**FYDA is sensitive to 200 μM copper, nickel, and zinc showing 30-, 70-, and 350-fold increases in activity, respectively. Tn D189S exhibited only baseline activity against YLVGP**RGH**FYDA (or slightly above) for each case.

Tn N143H, E151H, D189S is activated by zinc to cleave AGP**Y**A**H**SS at a rate 150-fold higher than Tn D189S. The k_{cat} for hydrolysis of AGP**Y**A**H**SS by Tn N143H, E151H, D189S with 200 μM Ni^{2+} is 20 ± 4 min^{-1} and the K_m = 1100 ± 400 μM, yielding a k_{cat}/K_m of 0.020 ± 0.004 μM^{-1} min^{-1}. In the presence of 200 μM zinc, k_{cat} = 275 ± 60 min^{-1} and K_m = 1300 ± 590 μM, yielding a k_{cat}/K_m of 0.24 ± 0.08 μM^{-1} min^{-1}. The 10-fold increase in activity with zinc relative to nickel is reflected in k_{cat}, not K_m. The zinc-activated k_{cat}/K_m of Tn N143H, E151H, D189S for this substrate is 65% of chymotrypsin activity on the same peptide, 0.37 ± 0.07 μM^{-1} min^{-1} (Willett et al., 1995). This triple mutant represents a 150-fold enhancement of metal-assisted specificity toward a tyrosine peptide bond over the previous double-mutant design, Tn N143H, E151H.

Figure 5b illustrates the results of metal-activated hydrolysis by Tn N143H, E151H of YLVGP**RGH**FYDA. Insufficient amounts of the peptide were available to determine k_{cat} and K_m values, so the relative activities are measured as the initial rate of hydrolysis (V_i) of the peptide under the given conditions. Comparison of hydrolysis rates (data not shown) of YLVGP**RGH**FYDA and AGP**YAH**SS in the presence of 200 μM zinc by Tn N143H, E151H, D189S shows that they are within 2-fold of each other, demonstrating the loss of activity against Arg at P_1 by removal of Asp

at position 189 in trypsin. Furthermore, hydrolysis of YLVGP**RGH**FYDA by Tn N143H, E151H, D189S plus 200 μM zinc is within 10-fold of the activity observed by Tn N143H, E151H, which possesses a wild-type S_1 subsite. In contrast to activity against AGP**YAH**SS, YLVGP**RGH**-FYDA hydrolysis is activated by copper as well as nickel and zinc. Copper activates activity 30-fold above background, nickel by 70-fold, and zinc by 350-fold. The control experiment using Tn D189S shows that none of the metals activate hydrolysis appreciably.

Analysis of Tn N143H, E151H/Ec A86H Crystal Contents. SDS−PAGE analysis of several crystals showed that they are an equimolar complex of trypsin and ecotin and that some proteolysis had occurred during the crystallization process. This is not surprising as Tn N143H, E151H possesses wild-type levels of activity against nominal trypsin substrates, and the crystallization takes place at pH 8.0 where trypsin is optimally active. Although there was no detectable degradation product in the purified stock of enzyme, there was an extra band in the sample of the crystal complex which migrated at approximately 12 kDa on a reducing SDS−polyacrylamide gel. To confirm that trypsin autolysis products were being generated, the 12 kDa band was blotted onto PVDF membrane and sequenced. The N-terminal sequence (data not shown) revealed a major sequence, NH_2-VATVA. This is the sequence that immediately follows Arg 117 (Craik et al., 1984), confirming that autolysis was occurring at Arg 117 in Tn N143H, E151H during crystallization. When the electrophoresis was repeated under nonreducing conditions, the 12 kDa band was not present, indicating that this trypsin fragment was bound to the rest of the molecule by the Cys 22−Cys 157 disulfide bond, thereby allowing the enzyme to maintain its structure during crystallization and data collection. Crystallization trials with Tn N193H, E151H, D189S complexed with Ec A86H did not yield crystals. Therefore, X-ray structural analysis was performed using Tn N143H, E151H complexed to Ec A86H. This complex was judged adequate for structural determination under the assumption that a mutation in the P_1 pocket of trypsin (Tn D189S) would not significantly perturb the structure of the $P_2'-S_2'$ interface.

The accompanying paper describes the X-ray crystallographic structure analysis of the four cases of interest for interpreting these kinetic results: apo (without metal), copper, nickel, and zinc structures for Tn N143H, E151H complexed to Ec A86H.

DISCUSSION

Design Improvement for Metal-Assisted Specificity. One of the advantages of using trypsin as a model system is the availability of high-resolution structural as well as detailed kinetic information. We have used this information to alter multiple amino acids, with the goal of increasing the metal-assisted specificity toward a target substrate. Removal of the negative charge in the bottom of the primary specificity pocket to create Tn N143H, E151H, D189S has resulted in a 150-fold improvement in the hydrolysis rate of the octapeptide AGP**Y**−**AH**SS in the presence of zinc. This triple mutant is capable of cleaving a tyrosine substrate at 65% of the chymotrypsin-catalyzed rate on the same substrate. A 350-fold rate increase in activity was observed in the presence of zinc for cleavage of YLVGP**R**−**GH**FYDA by Tn N143H, E151H, D189S relative to the rate with no metal present. This rate of hydrolysis is within 10-fold of the rate catalyzed by Tn N143H, E151H which possesses a wild-type S_1 subsite. These results demonstrate that, by utilizing both the S_1 and S_2' subsites on the enzyme as engineering targets, the substrate specificity of trypsin can be delocalized from a stringent P_1 specificity to an enzyme that also requires a histidine at P_2' in addition to zinc. These three point mutations in trypsin N143H, E151H, D189S allow hydrolysis of a tyrosine peptide bond with minimal loss of catalytic efficiency relative to chymotrypsin. The ecotin A86H inhibition constant, K_i, was not used as an indicator of metal-activated P_2'-His binding because the extensive contacts made in the remainder of the trypsin−ecotin interface would preclude any small effect that may have been observed at the $P_2'-S_2'$ interface.

The order of activating potential of the three metal ions used, Zn > Ni > Cu, can be explained partially by a combination of two factors: preferred geometry (Glusker, 1991) and intrinsic affinity of metal ion for histidine (Martell & Smith, 1974). Zinc prefers a tetrahedral arrangement of ligands as was designed for the site. Nickel prefers a square planar or sometimes tetrahedral geometry for tetracoordinate complexes. Copper prefers a square planar geometry. The affinity for histidine of these metal ions is Cu > Ni > Zn. The catalytic efficiency of this enzyme−substrate pair directly correlates with the preference of the metal for tetrahedral geometry and is inversely proportional to the affinity of the metal ion for histidine. These two factors taken together suggest a hypothesis for the observed kinetic effect. Given that the metal binding site is partially made by the leaving group of the acylation reaction in the course of the catalytic scheme (P_2'-His), it may be that the tighter binding metal creates a product−dissociation limiting case, while the metal ion that prefers tetrahedral geometry allows for the best alignment of the substrate, causing increased catalysis due to proper catalytic register of the substrate (Craik et al., 1985). Of course, the rationalization is more complicated because there are also metal−substrate and metal−buffer equilibria, nonspecific interactions of metal and enzyme, and protein dynamics to consider, but the simple explanation above is reasonable in light of the results of the X-ray crystallography (see accompanying paper). These results indicate that delocalizing the substrate binding energy from primarily the P_1 position observed in trypsin to the P_1 and P_2' positions found in Tn N143H, E151H, D189S is an effective way to alter substrate specificity in a protease. The substrate binding energy has been delocalized by crippling the P_1 pocket of trypsin through removal of the negative charge at position 189 and by adding a productive binding interaction at P_2' through an intermolecular metal binding site. In this way, transition metal ions reconstitute Tn N143H, E151H, D189S activity to 65% of chymotrypsin activity against a tyrosine substrate and to 10% of trypsin activity against an arginine substrate. This result compares with the method of loop-swapping used to create chymotrypsin specificity in trypsin (Hedstrom et al., 1994). By swapping in residues that comprise the S_1 subsite and two loops flanking the S_1 subsite of chymotrypsin into trypsin (a total of 12 mutations), a protease was created that possessed 15% of chymotrypsin activity. However, those studies were carried out with synthetic substrates which lack prime-side binding interactions, and so they may not have

observed possible higher catalytic efficiency against peptide substrates due to those extended binding subsite interactions. The results here suggest a general method for engineering protease specificity. We have demonstrated the ability to engineer individual subsite interactions to allow delocalization of primary specificity to more than one binding pocket with additive effects from each subsite interaction, which is a significant step toward the goal of designing substrate specificity.

REFERENCES

Abrahmsen, L., Tom, J., Burnier, J., Butcher, K. A., Kossiakoff, A., & Wells, J. A. (1991) *Biochemistry 30*, 4151−4159.

Arnold, F. H. (1993) *FASEB J. 7*, 744−749.

Braxton, S., & Wells, J. A. (1992) *Biochemistry 31*, 7796−7801.

Brinen, L. S., Willett, W. S., Craik, C. S., & Fletterick, R. J. (1996) *Biochemistry 35*, 5999−6009.

Carter, P., & Wells, J. A. (1987) *Science 237*, 394−399.

Chakrabarti, P. (1990) *Protein Eng. 4*, 57−63.

Christianson, D. W., & Alexander, R. S. (1989) *J. Am. Chem. Soc. 111*, 6412−6419.

Corey, D. R., Willett, S., Coombs, G. S., & Craik, C. S. (1995) *Biochemistry 34*, 11521−11527.

Craik, C. S., Choo, Q. L., Swift, G. H., Qinto, C., MacDonald, R. J., & Rutter, W. J. (1984) *J. Biol. Chem. 259*, 14255−14264.

Craik, C. S., Largman, C., Fletcher, T., Roczniak, S., Barr, P. J., Fletterick, R., & Rutter, W. J. (1985) *Science 228*, 291−297.

Glusker, J. P. (1991) *Adv. Protein Chem. 42*, 1−76.

Hedstrom, L., Perona, J. J., & Rutter, W. J. (1994) *Biochemistry 33*, 8757−8763.

Higaki, J. N., Haymore, B. L., Chen, S., Fletterick, R. J., & Craik, C. S. (1990) *Biochemistry 29*, 8582−8586.

Kunkel, T. A. (1985) *Proc. Natl. Acad. Sci. U.S.A. 82*, 488−492.

Martell, A. D., & Smith, R. M. (1974) *Critical Stability Constants*, Plenum Press, New York.

McGrath, M. E., Hines, W. M., Sakanari, J. A., Fletterick, R. J., & Craik, C. S. (1991) *J. Biol. Chem. 266*, 6620−6625.

McGrath, M. E., Erpel, T., Bystroff, C., & Fletterick, R. J. (1994) *EMBO J. 13*, 1502−1507.

McPherson, A. (1989) *Preparation and Analysis of Protein Crystals* Robert E. Kreiger Publishing Co., Malabar, FL.

Paoni, N. F., Chow, A. M., Pena, L. C., Keyt, B. A., Zoller, M. J., & Bennett, W. F. (1993) *Protein Eng. 6*, 529−534.

Perona, J. J., & Craik, C. S. (1995) *Protein Sci. 4*, 337−360.

Perona, J. J., Hedstrom, L., Wagner, R. L., Rutter, W. J., Craik, C. S., & Fletterick, R. J. (1994) *Biochemistry 33*, 3252−3259.

Ponder, J. W., & Richards, F. M. (1987) *J. Mol. Biol. 193*, 775−791.

Wang, C. I., Yang, Q., & Craik, C. S. (1995) *J. Biol. Chem. 270*, 12250−12256.

Willett, W. S., Gillmor, S. A., Perona, J. J., Fletterick, R. J., & Craik, C. S. (1995) *Biochemistry 34*, 2172−2180.

BI9530191